Desalination and Water Treatment
www.deswater.com

doi: 10.5004/dwt.2018.21955

108 (2018) 253–267
March

Removal of Cd^{2+} and Hg^{2+} from aqueous solutions by adsorption onto nitrogen-functionalized carbon nanotubes

Oluwaseun A. Oyetade, Vincent O. Nyamori, Sreekantha B. Jonnalagadda, Bice S. Martincigh*

School of Chemistry and Physics, University of KwaZulu-Natal, Westville Campus, Private Bag X54001, Durban 4000, South Africa, Tel. +27 31 260 1394; Fax: +27 31 260 3091; email: martinci@ukzn.ac.za (B.S. Martincigh), Tel. +27 74 650 4646; email: sennyoyez@yahoo.com (O.A. Oyetade), Tel. +27 31 260 8256; email: nyamori@ukzn.ac.za (V.O. Nyamori), Tel. +27 31 260 7325; email: jonnalagaddas@ukzn.ac.za (S.B. Jonnalagadda)

Received 6 September 2017; Accepted 24 January 2018

ABSTRACT

The efficiency of nitrogen-functionalized multiwalled carbon nanotubes (MWCNT-ttpy) for the removal of Cd^{2+} and Hg^{2+} from aqueous solutions was investigated and compared with their uptake on acid-functionalized multiwalled carbon nanotubes (MWCNT-COOH). Batch adsorption experiments investigating the influence of pH, contact time, adsorbent dose, metal ion concentration and adsorbate temperature were performed to determine the best sorption conditions for their removal. The experimental data obtained for both adsorbates were best described by the pseudo-second-order model, indicating a bimolecular chemical interaction between active sites on the adsorbents and the metal ion species. The Langmuir and Sips isotherm models best described the equilibrium data obtained for both sorbates. For Cd^{2+}, an uptake (q_m) of 10.41 mg g^{-1} for MWCNT-COOH was achieved and 41.51 mg g^{-1} for MWCNT-ttpy. An increase in Hg^{2+} uptake was also obtained for MWCNT-ttpy of 36.13 mg g^{-1} compared with 33.89 mg g^{-1} for MWCNT-COOH. Hence, MWCNT-ttpy proved to be more effective towards the removal of both adsorbates, relative to MWCNT-COOH. Desorption experiments conducted by using HCl as eluent afforded excellent recovery of sorbates and regeneration of sorbents, thus, increasing the chances of reutilization of sorbents. Hence, the application of MWCNT-ttpy as a potential sorbent for effluent and wastewater treatment is feasible and should be further explored for water pollution control.

Keywords: Multiwalled carbon nanotubes; Kinetics; Isotherm; Cadmium; Mercury

1. Introduction

The increase in the contamination of water supplies with toxins, such as heavy metals, has intensified in recent times due to the proliferation of urbanization and industrialization [1,2]. Industrial activities from battery manufacturing, electroplating, tanning and mining, produce effluents containing a variety of pollutants, especially metal ions in large amounts. Therefore, metal ions are largely distributed into natural waters through the indiscriminate discharge of industrial effluents into these water bodies [3–5].

Heavy metal contamination is one of the most significant environmental challenges and this is due to their solubility in water, and mobility, accumulation and persistence in the environment [4,6]. Cadmium and mercury are regarded as one of the most poisonous pollutants [4,7], whose intake, even at low concentrations, results in several long-term health effects in man, wildlife and aquatic life [8]. The pathway through which Cd^{2+} enters into the environment is via the discharge of wastes generated from smelting, alloy production, electroplating, batteries, mining and refinery operations [3,9].

* Corresponding author.

An intake of Cd^{2+} can result in damage of the lungs, kidneys and pancreas, and may also lead to various cardiovascular diseases [3,4,10]. Due to its ability to bioaccumulate in man, Cd^{2+} may persist in the human system for a period of 10 years [8,11]. Based on these consequences, concentrations of 0.005 and 0.003 mg dm^{-3} were recommended by the United States Environmental Protection Agency (US EPA) and the World Health Organization (WHO), respectively, as the maximum permissible limits of Cd^{2+} in drinking water [9,11–13].

Additionally, the intake of mercury and its associated compounds can lead to several developmental and neurological changes in living organisms [14]. Exposure to mercury is considered toxic to man, resulting in blood vessel congestion, kidney and lung dysfunction, cancerous, teratogenic and mutagenic diseases and, in extreme cases, may lead to death [14–16]. The release of Hg^{2+} into the environment is associated with vapours produced from volcanic eruptions and weathering of rocks [7], and emissions from coal-burning power plants and waste incinerators [17–19]. The most common discharge route of Hg^{2+} into aqueous solutions is the release of wastewater produced from paint, pulp, paper, fertilizer and chloralkali manufacturing industries into receiving water streams [7,15]. The mercury poisoning reported in Minamata, Japan, was initiated by the release of methylmercury-contaminated wastewater, produced from an industrial factory into water bodies in 1956 [7,15,16]. This resulted in the bioaccumulation of mercury in aquatic life. Its subsequent ingestion by man resulted in acute aftermaths such as coma and death. To this end, a concentration of 0.006 mg dm^{-3} was recommended by WHO as the maximum permissible limit of Hg^{2+} in drinking water [12,13].

In spite of the restraints on the use of Cd^{2+} and Hg^{2+} by the Restriction of Hazardous Substance Directives (RoHS) [20], these toxic metals are still employed for applications such as electrical and lightening equipment in industries [20] and often used in thermometers and manometers in the laboratory. Hence, the generation of contaminated wastewater polluted by these toxins still exists. The treatment of wastewater is therefore of utmost importance before it is discharged into receiving streams.

Several techniques such as chemical precipitation [21], electrodeposition [22,23], reverse osmosis [24], coagulation [25], ion-exchange [26] and adsorption [1,6,7,27,28] have been employed for heavy metal removal from wastewater. The efficacy of some of these techniques for metal ion removal has been poor [3,4,15]. However, adsorption is a promising method for metal ion removal from wastewater due to its simplicity, cost-effectiveness and the ability to regenerate spent adsorbents for reuse [3,9,11]. Adsorbents are easily handled [29], hence, the usage of sorbents such as activated carbon [30], resins [31], biochars [4], bagasse [32], rice husk [33] and clay [10,34], among many others, has been employed for Cd^{2+} and Hg^{2+} removal. Slow sorption processes, low adsorption capacity and inability to regenerate sorbents for reuse are some drawbacks attributed to the use of some conventional sorbents [35]. Hence, there is a need for the development of a fast, effective and efficient sorbent for the remediation of wastewater contaminated with either Cd^{2+} or Hg^{2+}.

A growing research interest in the utilization of shaped carbon nanostructured materials as adsorbents has led to the application of multiwalled carbon nanotubes (MWCNTs) for pollutant removal in environmental sciences. MWCNTs possess remarkable physical and chemical properties with extraordinary thermal stability, and high porosities and surface areas available for adsorption [36,37]. Although MWCNTs are highly hydrophobic in nature, their surfaces are easily functionalized to contain a number of functional groups, which serve as active sites for the removal of targeted pollutants from aqueous solutions. MWCNTs have been successfully applied for the removal of a variety of pollutants such as perfluorinated compounds [38], polyaromatic compounds [39], dyes [35,40] and phenol [41], among many. Metal ions, such as Cd^{2+} and Hg^{2+}, have also been removed from wastewater by using MWCNT-containing adsorbents [2,9,11]. For increased application in a practical sense, the adsorption efficiency of MWCNTs needs to be improved to favour the effective and efficient removal of Cd^{2+} and Hg^{2+} from wastewater.

To overcome this hurdle, 4′-(4-hydroxyphenyl)-2,2′:6′,2″-terpyridine (HO-Phttpy) was employed as a modifier for further functionalization of acid-functionalized MWCNTs (MWCNT-COOH). This process aims to improve the surface area and pore volume of the adsorbent, and hence increase the number of chelating sites available for adsorption. In this study, we report for the first time, the efficiency of 4′-(4-hydroxyphenyl)-2,2′:6′,2″-terpyridine functionalized MWCNT (MWCNT-ttpy) for the removal of Cd^{2+} and Hg^{2+} from aqueous solutions through a series of batch experiments. The uptake of the two adsorbates onto MWCNT-ttpy was compared with the adsorption capacity of MWCNT-COOH. Also, the kinetics of adsorption and the equilibrium isotherms were investigated.

2. Experimental

2.1. Materials and chemicals

Cadmium metal powder (99.9%) was obtained from Thomas Baker Chemicals (Pvt) Ltd. (Mumbai, India), while mercury(II) nitrate-monohydrate ($Hg(NO_3)_2.H_2O$) and potassium chloride (KCl, 99.8%) were obtained from BDH Laboratory Supplies (Poole, England). Diphenyl carbazone was purchased from The British Drug Houses Ltd. (London, England). Sodium hydroxide (NaOH, 98%) was purchased from Merck Chemicals (Pty) Ltd. (Gauteng, South Africa) while chemicals such as sodium borohydride ($NaBH_4$) (99%), 4-hydroxybenzaldehyde (99%), 2-acetylpyridine (99%), indium bromide ($InBr_3$, 99%) and solvents such as absolute ethanol, *N*,*N*′-dimethylformamide (DMF, 99%), dimethyl sulphoxide-d_6 (DMSO-d_6, 99%) and triethylsilane (Et_3SiH, 97%) were purchased from Sigma-Aldrich (St. Louis, USA). Tetrahydrofuran (THF, 99%), chloroform (99%) and thionyl chloride ($SOCl_2$, 99%) were purchased from Merck Chemicals (Pty) Ltd. (Gauteng, South Africa) while aqueous ammonia (25%) was purchased from Associated Chemical Enterprises (Johannesburg, South Africa). Nitric (55%), sulphuric (98%) and hydrochloric acids (32%) were obtained from C.C. Imelmann Ltd. (Robertsham, South Africa). All materials and chemicals were of analytical grade and used as-received from suppliers without further purification. Pristine-MWCNTs (P-MWCNTs) (purity > 95%), synthesized by chemical vapour deposition (CVD), were obtained from Cheap Tubes Incorporation (Brattleboro, USA).

2.2. Synthesis of 4′-(4-hydroxyphenyl)-2,2′:6′,2″-terpyridine (HO-Phttpy)

The ligand was synthesized as reported by Oyetade et al. [42]. In brief, 2-acetylpyridine (2.423 g, 20.0 mmol) was added to 15 cm^3 of a 2:1 (v/v) mixture of ethanol and water containing 4-hydroxybenzaldehyde (1.221 g, 10.0 mmol). To the suspension, NaOH pellets (1.458 g, 26.0 mmol) and 30 cm^3 aqueous NH_3 were added and stirred continuously at room temperature for 8 h to yield a cream-coloured precipitate. The resulting mixture was filtered, the solid obtained was washed with deionized water (5 × 10 cm^3), followed by absolute ethanol (3 × 5 cm^3), to obtain the crude white product (508.8 mg, 42%).

2.3. Adsorbent preparation

2.3.1. Preparation of oxidized MWCNTs (MWCNT-COOH)

Oxidation of MWCNTs was carried out as reported by Santangelo et al. [43]. Pristine-MWCNTs (1.5 g) were placed in a round-bottomed flask containing 100 cm^3 of concentrated hydrochloric acid, and stirred for 4 h to remove residual metal impurities from the tubes. The resulting solution was filtered, and the solid washed with deionized water until a neutral pH was obtained. The sample obtained was dried in a vacuum oven at 80°C overnight and stored in a desiccator for future analysis. The purified MWCNTs were then oxidized by using a mixture of sulphuric and nitric acids in a volume ratio of 1:3, and refluxed at 80°C for 12 h. The resulting solution was diluted with deionized water, filtered, and the residue obtained was washed continuously with deionized water until a neutral pH was obtained.

2.3.2. Preparation of nitrogen-functionalized MWCNTs (MWCNT-ttpy)

Oxidized MWCNTs (150 mg) were dispersed in 30 cm^3 of a solution containing a 20:1 (v/v) mixture of $SOCl_2$ and DMF, and then refluxed at 70°C for 24 h [44]. The resulting mixture was filtered, and the solid obtained was washed with deionized water until a neutral pH was achieved. Acylated MWCNTs (100 mg) were added to 100 mg of HO-Phttpy in 20 cm^3 of dry THF with the addition of 2–5 drops of glacial acetic acid. The suspension was refluxed at 64°C for 24 h under an inert atmosphere of argon. The suspension was filtered, and the solid obtained was washed with THF and dried in a vacuum oven.

The sample obtained (100 mg) was added to freshly distilled chloroform (30 cm^3), $InBr_3$ (10.6 mg, 0.03 mmol) and Et_3SiH (380 μL, 2.4 mmol). The suspension was stirred and refluxed at 60°C for 1 h under an inert atmosphere of argon. The resulting mixture was filtered and the solid washed with chloroform, followed by water until a neutral pH was obtained. Evidence of the successful preparation of MWCNT-COOH and MWCNT-ttpy was obtained by various characterization techniques such as electron microscopy (scanning and transmission), Fourier transform infrared (FTIR) and Raman spectroscopy, thermogravimetric analysis, elemental analysis and Brunauer, Emmett and Teller (BET) surface area analysis.

2.4. Metal analysis procedure

2.4.1. Equipment

A PerkinElmer Optima 5300 DV inductively coupled plasma-optical emission spectrophotometer (ICP-OES) was used to measure the initial and final concentrations of Cd^{2+} in solution at a wavelength of 228.8 nm. Mercury analysis was performed on a PerkinElmer AAnalyst 200 atomic absorption spectrometer fitted with a hollow cathode lamp operated at a wavelength of 253.7 nm. The system was also equipped with a PerkinElmer mercury hydride system (MHS 15).

2.4.2. Preparation of adsorbate solutions

A stock solution of Cd^{2+} was prepared by dissolving 1 g of cadmium metal in 20 cm^3 of concentrated HCl acid and 3–5 drops of HNO_3 acid. The solution was then made up to the mark in a 1,000 cm^3 volumetric flask with deionized water. Working solutions of desired concentrations were made by dilution of this stock solution.

About 1.713 g of $Hg(NO_3)_2.H_2O$ was dissolved in 10 cm^3 of nitric acid and diluted to the mark in a 500 cm^3 volumetric flask with deionized water. This solution was standardized against KCl by using diphenylcarbazone indicator [45]. A solution of Hg^{2+} with a concentration of 1,000 mg dm^{-3} was prepared by measuring the required volume of the $Hg(NO_3)_2.H_2O$ stock solution and diluting to the mark, in a 1,000 cm^3 volumetric flask with deionized water. Working solutions of Hg^{2+} were prepared from the 1,000 mg dm^{-3} $Hg(NO_3)_2.H_2O$ solution by dilution to obtain the desired concentration.

2.4.3. Calibration of spectrophotometers

The ICP-OES and cold vapour atomic absorption spectrophotometer (CVAAS) were calibrated for Cd^{2+} and Hg^{2+} analysis, respectively, by preparing standard solutions of Cd^{2+}/Hg^{2+} with concentrations within the range of 0–100 mg dm^{-3} at each time of analysis. Calibration plots were obtained in these ranges and the initial and final concentrations of Cd^{2+}/Hg^{2+} in the samples were estimated from these plots. For the CVAAS analysis of mercury, the reductant was a 0.8 mol dm^{-3} $NaBH_4$ solution, which was prepared by dissolving a known amount of the salt in 1% NaOH solution, and thereafter diluted to the mark with the same solution in a 200 cm^3 volumetric flask.

2.5. Batch adsorption studies

The influence of adsorption parameters, such as pH, contact time, adsorbent dose, initial metal ion concentration and temperature, was investigated through batch adsorption experiments for the removal of Cd^{2+} and Hg^{2+} onto MWCNT-COOH and MWCNT-ttpy. Experiments were conducted sequentially to obtain the best experimental conditions for the adsorption of Cd^{2+} and Hg^{2+} from aqueous solutions. Working solutions of Cd^{2+} and Hg^{2+} with concentrations of 100 and 50 mg dm^{-3}, respectively, were prepared from the respective stock solutions.

Adsorption experiments were conducted by measuring 25 cm^3 aliquots of either a Cd^{2+} or Hg^{2+} solution into 100 cm^3 polypropylene plastic vials, and conditioned to obtain the desired pH with the addition of appropriate amounts of

0.1 mol dm^{-3} NaOH or HNO_3 solution. A mass of 50 mg of each adsorbent was added into the solution and agitated in a thermostated water bath preset at 20°C for 24 h. After agitation, the solutions were filtered, and the final concentrations of Cd^{2+} or Hg^{2+} determined by ICP-OES and CVAAS, respectively. The amount of metal ion adsorbed on each sorbent was estimated from the difference between the initial and equilibrium metal ion concentrations. The adsorption capacity (q_e) of Cd^{2+} and Hg^{2+} was calculated from Eq. (1):

$$q_e = \left(\frac{C_i - C_{eq}}{m}\right) \times V \quad (1)$$

where C_i is the initial adsorbate concentration (mg dm^{-3}), C_{eq} is the equilibrium concentration of adsorbate (mg dm^{-3}), q_e is the adsorption capacity (mg g^{-1}), m is the mass of adsorbent (g) and V is the volume (dm^3) of the adsorbate solution used. The percentage removal (% adsorbed) of Cd^{2+} and Hg^{2+} was calculated according to Eq. (2):

$$\%\ \text{adsorbed} = \left(\frac{C_i - C_{eq}}{C_i}\right) \times 100 \quad (2)$$

2.5.1. Kinetics, isotherm and thermodynamic studies

The equilibration time of the adsorption process for each metal ion was determined by means of kinetic experiments. This was carried out by weighing about 50 mg of each sorbent into 100 cm^3 polypropylene bottles, containing 25 cm^3 aliquots of either a Cd^{2+} or Hg^{2+} solution. The solutions were conditioned to obtain the desired pH by adding appropriate amounts of 0.1 mol dm^{-3} NaOH or HNO_3 solution, and thereafter the bottles were placed in a thermostated water bath at 20°C. These samples were agitated for different time intervals in the range of 5–1,440 min. After the predetermined time intervals, the samples were filtered by gravity and the concentration of Cd^{2+} or Hg^{2+} determined by ICP-OES or CVAAS, respectively. The experimental adsorption data obtained were applied to the pseudo-first-order, pseudo-second-order, intraparticle diffusion and Elovich kinetics models as given in Table 1.

Adsorption isotherms were obtained by using varying concentrations of Cd^{2+} or Hg^{2+} ranging from 10 to 100 mg dm^{-3}, at a constant pH of 5.5 and 6.0, respectively. Aliquots of 25 cm^3 were mixed with 50 mg of each adsorbent and agitated in a thermostated shaking water bath for 24 h. The effect of temperature on the adsorption of Cd^{2+} was investigated at temperatures of 293, 303, 313 and 318 K, while similar experiments for Hg^{2+} were only conducted at 293 and 303 K, due to the volatility of Hg^{2+}. The experimental adsorption equilibrium data were analyzed by various two- and three-parameter isotherm models, such as the Langmuir, Freundlich, Temkin, Dubinin–Radushkevich, Sips, Toth, Redlich–Peterson and Khan models, as given in Table 2.

Table 1
Kinetics models used for the adsorption of Cd^{2+} and Hg^{2+}

Model	Equation[a]	Parameters	References
Pseudo-first-order	$q_t = q_{eq}(1 - e^{-k_1 t})$	$q_{eq}\ k_1$	[46–48]
Pseudo-second-order	$q_t = \frac{k_2 q_{eq}^2 t}{1 + k_2 q_{eq} t}$	$k_2\ q_{eq}$	[46,48,49]
Elovich	$q_t = \frac{1}{\beta}\ln(\alpha\beta) + \frac{1}{\beta}\ln t$	$\alpha\ \beta$	[50]
Intraparticle diffusion	$q_t = k_{id}\sqrt{t} + l$	$k_{id}\ l$	[51]

[a]q_t – quantity of adsorbate adsorbed at time t (mg g^{-1}); q_{eq} – quantity of adsorbate adsorbed at equilibrium (mg g^{-1}); α – adsorption rate constant (mg g^{-1} min^{-1}); β – desorption rate constant (g mg^{-1}); k_1 – pseudo-first-order rate constant (min^{-1}); k_2 – pseudo-second-order rate constant (g mg^{-1} min^{-1}); k_{id} – intraparticle diffusion rate constant (mg g^{-1} min$^{0.5}$) and l – is a constant related to the boundary layer thickness.

Table 2
Isotherm models used for the adsorption of Cd^{2+} and Hg^{2+}

Isotherm	Equation[a]	Parameters	References
Langmuir	$q_{eq} = \frac{q_m b C_{eq}}{1 + b C_{eq}}$	$q_m\ b$	[52]
Freundlich	$q_{eq} = K_F C_{eq}^{1/n}$	$K_F\ n$	[53]
Temkin	$q_{eq} = \frac{RT}{b_T}\ln\left(A_T C_{eq}\right)$	$b_T\ A_T$	[54]
Dubinin–Radushkevich	$q_{eq} = q_m e^{-\beta\varepsilon^2}$ $\varepsilon = RT\ln\left(1 + \frac{1}{C_{eq}}\right)$	$q_m\ \beta$	[55]
Sips	$q_{eq} = \frac{b q_m C_{eq}^{1/n}}{1 + b C_{eq}^{1/n}}$	$q_m\ b\ n$	[56]
Toth	$q_{eq} = \frac{q_m C_{eq}}{\left(\frac{1}{K_T} + C_{eq}^{n_T}\right)^{1/n_T}}$	$q_m\ K_T\ n_T$	[57]
Redlich–Peterson	$q_{eq} = \frac{K_{RP} C_{eq}}{1 + a_{RP} C_{eq}^{g}}$	$K_{RP}\ a_{RP}\ g$	[58]
Khan	$q_{eq} = \frac{q_m b_K C_{eq}}{\left(1 + b_K C_{eq}\right)^{a_K}}$	$q_m\ a_K\ b_K$	[59]

[a]q_{eq} – adsorption capacity (mg g^{-1}); C_{eq} – equilibrium concentration of adsorbate in solution (mg dm^{-3}); q_m – maximum monolayer capacity (mg g^{-1}); b – Langmuir isotherm constant (dm^3 mg^{-1}); K_F – Freundlich isotherm constant (mg g^{-1})(dm^3 mg^{-1})^n; n – adsorption intensity; b_T – Temkin isotherm constant; A_T – Temkin isotherm equilibrium binding constant (dm^3 g^{-1}); β – Dubinin–Radushkevich isotherm constant (mol^2 kJ^{-2}); K_T – Toth isotherm constant (mg g^{-1}); n_T – Toth isotherm constant; K_{RP} – Redlich–Peterson isotherm constant (dm^3 g^{-1}); a_{RP} – Redlich–Peterson isotherm constant; g – Redlich–Peterson isotherm exponent; a_K – Khan isotherm exponent and b_K – Khan isotherm constant.

Thermodynamic parameters, such as change in Gibbs energy ($\Delta G°$), change in enthalpy ($\Delta H°$) and change in entropy ($\Delta S°$), were also calculated over the studied temperature ranges.

2.6. Desorption experiments

After conducting adsorption experiments with a 50 mg dm^{-3} solution of Cd^{2+} or Hg^{2+} by using a 50 mg dose of each adsorbent, the loaded adsorbents were separated from the suspensions by filtration and the metal ion concentration in the filtrates was determined by using the appropriate previously described techniques. The collected sorbents were washed with deionized water to remove unadsorbed metal ions and dried in a vacuum oven at 80°C. Desorption experiments were then conducted by agitating 50 mg of the metal loaded-adsorbent with 25 cm^3 of 0.1 mol dm^{-3} HCl for 30 min. The mixture was then filtered and the concentration of the desorbed metal ions in the filtrates was determined as described before. The percentage of metal desorbed was calculated from Eq. (3):

$$\text{Percentage desorption}(\%) = \frac{\text{Released metal ion concentration}}{\text{Initial metal ion concentration}} \times 100 \quad (3)$$

2.7. Data analysis

The data obtained were fitted to the isotherm and kinetics models by means of the nonlinear regression routine (*nls*) in the R statistical computing environment [60]. The R statistical software takes into account the minimization of the sum of squared residuals (SSR) and the residual squared errors (RSE). A comparison of all SSR and RSE values was done and the adequacy of the models was assessed from the value with the lowest SSR.

Table 3
Textural characterization of synthesized nanomaterials

Entry	Adsorbents	Surface area ($m^2\ g^{-1}$)	Pore volume ($cm^3\ g^{-1}$)	Pore diameter (nm)
1	P-MWCNT	108.8	0.494	18.44
2	MWCNT-COOH	126.8	0.692	22.95
3	MWCNT-ttpy	189.2	1.252	27.26

3. Results and discussion

3.1. Characterization of adsorbents

The characterization of the two adsorbents, MWCNT-COOH and MWCNT-ttpy, has been previously reported by Oyetade et al. [42]. Some pertinent characteristics of the adsorbents are presented in Tables 3 and 4. As can be seen in Table 3, the surface area and pore volume of MWCNT-ttpy are larger than those obtained for MWCNT-COOH. Also, MWCNT-ttpy contains a larger number of functional groups per unit mass than MWCNT-COOH (Table 4). These properties demonstrate that both adsorbents may be suitable for metal ion sorption from aqueous solutions.

3.2. Batch adsorption experiments

Batch adsorption experiments were conducted to investigate the optimum conditions for Cd^{2+} and Hg^{2+} removal from aqueous solutions. In this section, the influence of pH, contact time, adsorbent dose, initial metal ion concentration and adsorbate temperature is presented and the results are discussed. Kinetics, isotherm and thermodynamic studies were also performed to understand the mechanisms involved in the removal of the targeted metal ions from aqueous solutions.

3.2.1. Effect of pH

Metal ion adsorption is significantly influenced by the solution pH, since it controls the distribution of species, surface charges and also the degree of ionization of the sorbent [7]. The influence of pH on the sorption of Cd^{2+} and Hg^{2+} onto MWCNT-COOH and MWCNT-ttpy from aqueous solutions was studied over a pH range of 1–10. Fig. 1 shows that the percentage Cd^{2+} and Hg^{2+} adsorbed by both adsorbents increases as the solution pH becomes more basic. The extent of Cd^{2+} removal by MWCNT-COOH increased steadily from 9.5% to 59.0%, while higher removal efficiencies of 22.0% to 99.2% were obtained with MWCNT-ttpy over the same pH range (Fig. 1(a)). Similarly, an increase in Hg^{2+} removal onto MWCNT-COOH from 55.8% to 85.9%, and from 83.0% to 88.0% by MWCNT-ttpy, was observed with increasing solution pH as shown in Fig. 1(b).

These observations signify that the sorption of Cd^{2+} and Hg^{2+} was greatly enhanced by the change in solution pH. A lower removal of adsorbates under acidic conditions can be attributed to increasing competition between hydrogen ions and metal cations in solution. Also, this phenomenon induces an electrostatic repulsion between the metal cations and positive charges on the adsorbent, resulting in a lower removal

Table 4
Surface chemistry of P-MWCNTs, MWCNT-COOH and MWCNT-ttpy determined by the Boehm titration method [42]

Adsorbents	Carboxyl ($mmol\ g^{-1}$)	Lactonic ($mmol\ g^{-1}$)	Phenolic ($mmol\ g^{-1}$)	Total acidic groups ($mmol\ g^{-1}$)	Total basic groups ($mmol\ g^{-1}$)
P-MWCNTs	0.136	0.014	0.114	0.264	0.145
MWCNT-COOH	0.719	0.104	0.401	1.224	0.226
MWCNT-ttpy	0.613	0.165	0.544	1.322	0.752

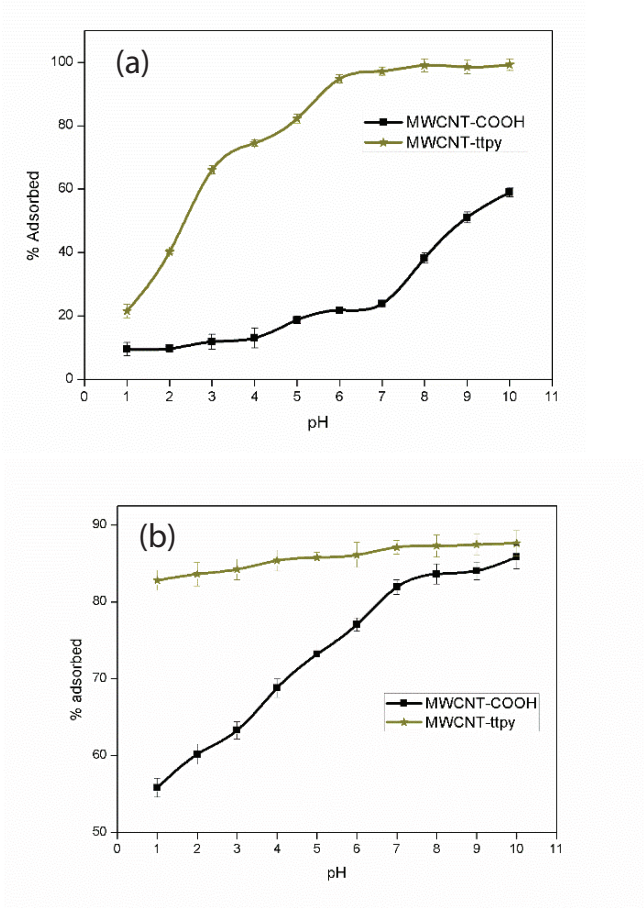

Fig. 1. Effect of pH on the adsorption of (a) Cd^{2+} and (b) Hg^{2+} by using MWCNT-COOH and MWCNT-ttpy (conditions: 25 cm^3 of 100 or 50 mg dm^{-3} of Cd^{2+}/Hg^{2+} solution, 24 h equilibration time, 50 mg adsorbent dose, agitation speed 150 rpm and temperature 20°C).

under acidic conditions. An increase in solution pH reduces the amount of hydrogen ions and increases the number of hydroxyl ions in solution. This process facilitates the sorption of both adsorbates via electrostatic attraction between cations and negative charges on the adsorbent. Similar trends were reported by Kadirvelu et al. [7], Shadbad et al. [61], Hadavifar et al. [62], Liang et al. [11] and Li et al. [9] involving the sorption of Cd^{2+} and Hg^{2+} onto MWCNT-containing sorbents. It is also worthy of note that the sorption of Cd^{2+} and Hg^{2+} onto MWCNT-ttpy was more pronounced than for MWCNT-COOH. This could be due to the affinity of the nitrogen-donor atoms in MWCNT-ttpy to preferentially bind to these two soft metal ions and the increased number of coordination sites available for chelation on this adsorbent. Hence, the increased metal ion uptake by MWCNT-ttpy could be attributed to metal ion coordination with the nitrogen-donor atoms on the surface of the adsorbent. These results are in agreement with the study reported by Hadavifar et al. [62], where amino- and thiol-functionalized MWCNTs proved more effective for Hg^{2+} removal than MWCNTs.

As shown in Fig. 2, various species of cadmium, such as $Cd(OH)^+$, $Cd(OH)_2$, $Cd(OH)_3$, $Cd(OH)_4$ and $Cd_4(OH)_4$, can be formed with increasing alkalinity of the solution. Similarly,

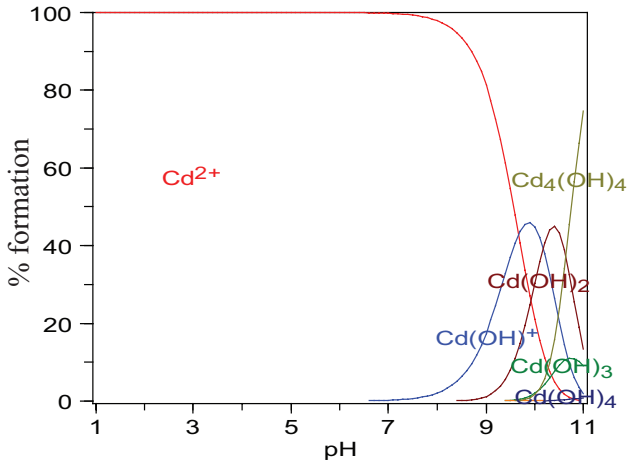

Fig. 2. Speciation of Cd^{2+} as a function of pH in aqueous solution. Numerical values of logβ for the metal hydroxides used in the calculation of the speciation curves were obtained from *Critical Stability Constants* compiled by Smith and Martell [63], and the speciation plot was obtained with the aid of HySS software [64].

in the case of mercury, species such as $Hg(OH)_2$, $Hg(OH)_3^-$ and $Hg(OH)^+$, may be formed under alkaline conditions. Hence, subsequent experiments were conducted at pH 5.5 and 6.0 for Cd^{2+} and Hg^{2+}, respectively, to avoid precipitation of metal ions accompanying adsorption in solution. At both these pH values, the metal ions exist as free metal ions available for adsorption and do not exists as hydrolyzed or protonated species.

3.2.2. *Effect of contact time*

To investigate the effect of contact time on the adsorption of Cd^{2+} and Hg^{2+} onto MWCNT-COOH and MWCNT-ttpy, adsorption experiments were agitated over a period of 5–1,440 min. Fig. 3 shows the percentage removal of Cd^{2+} and Hg^{2+} onto MWCNT-COOH and MWCNT-ttpy as a function of time. The figures reveal that the removal of both adsorbates increases with an increase in agitation time. Fig. 3(a) shows that equilibrium for the removal of Cd^{2+} was reached within 360 min for both adsorbates. However, the percentage adsorbed was four times greater for MWCNT-ttpy than for MWCNT-COOH. This signifies that MWCNT-ttpy is a better adsorbent for Cd^{2+} removal than MWCNT-COOH. This could be as a result of the introduction of nitrogen-donor atoms onto the adsorbent, which possess strong affinity towards cadmium metal ions. The soft Cd^{2+} ions will bind preferentially with the borderline pyridinyl-nitrogen donors in MWCNT-ttpy than the harder oxygen donors in MWCNT-COOH.

Similar trends were observed for the removal of Hg^{2+} onto MWCNT-COOH and MWCNT-ttpy (Fig. 3(b)). Fig. 3(b) shows that equilibrium was achieved at 240 and 120 min by using MWCNT-COOH and MWCNT-ttpy, respectively. However, the difference in the percentage adsorbed by the two adsorbents was not as marked for Hg^{2+} as it was for Cd^{2+} (Fig. 3(b) vs. (a)).

The rate of adsorption was rapid for the removal of Cd^{2+} and Hg^{2+} onto MWCNT-ttpy, attaining a percentage

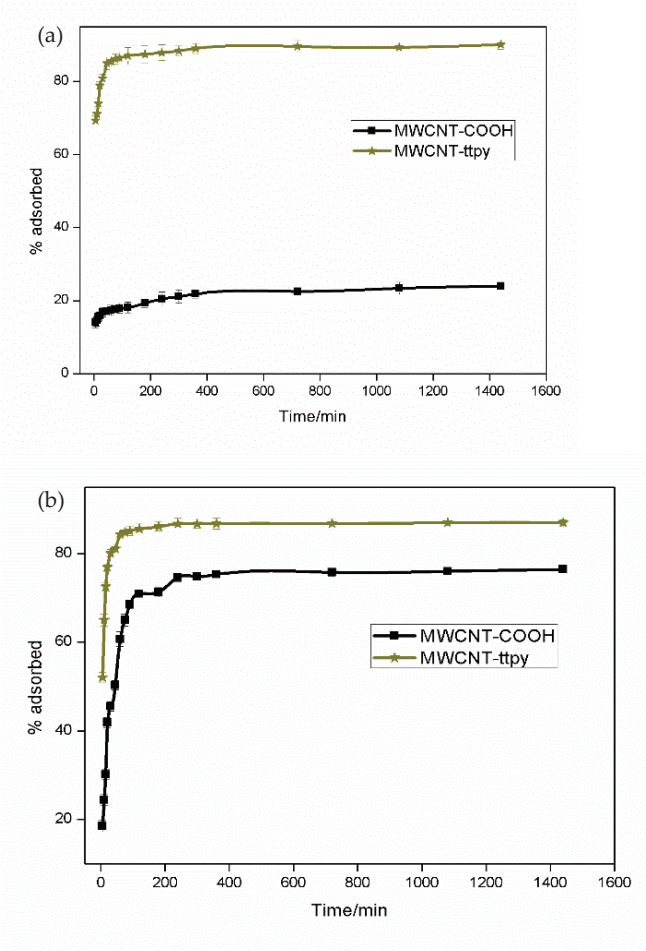

Fig. 3. Effect of contact time on the adsorption of (a) Cd^{2+} and (b) Hg^{2+} by using MWCNT-COOH and MWCNT-ttpy (conditions: 25 cm^3 of 100 or 50 mg dm^{-3} of Cd^{2+}/Hg^{2+} solution, 50 mg adsorbent dose, pH = 5.5 (Cd^{2+}) and pH = 6.0 (Hg^{2+}), agitation speed 150 rpm and temperature 20°C).

removal efficiency of 70% and 50%, respectively, after 5 min. The removal of the adsorbates onto both sorbents, however, slows down with increased contact time, due to saturation of the active sites on the adsorbents. Hence, the initial fast removal can be attributed to the availability of active sites which decrease with increase in time. In this study, all experiments were equilibrated for 24 h in order to ensure effective removal of adsorbates for higher concentrations.

3.2.2.1. Kinetics studies The mechanism of adsorption was investigated by modelling the kinetics data, to determine the rate-controlling step of the process. These experiments were conducted at fixed initial metal ion concentration, pH value, adsorbent dose, adsorbate volume and temperature. The experimental data collected at varying contact time, between 5 and 1,440 min, were analyzed through the kinetics models given in Table 1. A comparison of the stated models was done by using the non-linear regression (*nls*) routine in the R statistical computing software [60]. Table 5 presents the kinetics parameters obtained for both adsorption processes by using MWCNT-COOH and MWCNT-ttpy. The adequacy of the model which best describes the adsorption process was chosen based on the lowest values obtained for the SSR.

The adsorption of Cd^{2+} onto MWCNT-COOH and MWCNT-ttpy was better described by the Elovich and pseudo-second-order models, respectively (Table 5). On the other hand, the adsorption of Hg^{2+} onto both adsorbents was best described by the pseudo-second-order model. The pseudo-second-order model assumes that adsorption proceeds through a bimolecular chemical interaction between the adsorbate ions and the active sites on the adsorbents [65]. The adsorption of Hg^{2+} onto both adsorbents, and the removal of Cd^{2+} onto MWCNT-ttpy proceeded through this process. Hence, these adsorption processes were facilitated via bimolecular interactions between nitrogen- or oxygen-donor atoms and the metal cations. The Elovich model, on the other hand, is used to describe chemical sorption of gases onto solid surfaces. The mechanism of Cd^{2+} removal onto MWCNT-COOH therefore proceeded through the diffusion of adsorbate ions from the bulk solution to the surface of the adsorbent. Tofighy and Mohammadi [66], Liang et al. [11] and Vukovic et al. [67] also reported that Cd^{2+} removal by CNT-containing sorbents was better described by the pseudo-second-order model. However, they did not attempt to use the Elovich model. Also, the removal of Hg^{2+} produced similar trends as reported by Chen et al. [65], Shadbad et al. [61] and Kabbashi et al. [17].

The mechanism of adsorption can proceed via one or more of the following steps: (i) the transfer of solute from the bulk solution to the surface of the adsorbent, (ii) the transfer of solute from the bulk solution to the boundary film which surrounds the adsorbent surface (film diffusion), (iii) the solute transfer through the internal pores of the adsorbent (intraparticle diffusion) and (iv) the interaction between adsorbate molecules with the active sites on the external surface of the adsorbent. A plot of q_e vs. $\sqrt{t}$ gives an explanation into the processes controlling the adsorption. It is assumed that the process is multistep controlled if a linear plot is obtained which does not pass through the origin [68,69]. When a linear plot which passes through the origin is obtained, adsorption is assumed to proceed only by the intraparticle diffusion of adsorbates onto sites of the adsorbent [68]. All the plots obtained in this study were linear but did not pass through the origin, indicative that the adsorption of Cd^{2+} and Hg^{2+} was controlled by a series of steps. Hence, it could be inferred that the removal of Cd^{2+} and Hg^{2+} onto MWCNT-COOH and MWCNT-ttpy proceeded through intraparticle diffusion, and a number of other steps accompanying adsorption. Table 5 further demonstrates higher intraparticle diffusion constants (k_{id}) and boundary layer (l) values for MWCNT-ttpy than MWCNT-COOH for both adsorption processes. These results are indicative that adsorption was boundary-controlled, hence, an increase in the uptake of adsorbates was noticed with increase in l values. Similarly, Table 5 shows that higher l values were obtained for Cd^{2+} sorption by using both sorbents, compared with their corresponding values for Hg^{2+} sorption. This implied that both adsorbents had better affinity for the removal of Cd^{2+} than Hg^{2+}.

Table 5
Kinetics parameters for the adsorption of Cd^{2+} and Hg^{2+} on MWCNT-COOH and MWCNT-ttpy (conditions: 25 cm^3 of 100 mg dm^{-3} Cd^{2+} at pH 5.5, or 50 mg dm^{-3} Hg^{2+} at pH 6.0, 50 mg adsorbent dose, agitation speed 150 rpm and temperature 20°C)

Model	Parameter	Cd^{2+}		Hg^{2+}	
		MWCNT-COOH	MWCNT-ttpy	MWCNT-COOH	MWCNT-ttpy
Experimental	q_{meas}/mg g^{-1}	9.734	36.72	18.55	22.41
Pseudo-first-order	$k_1/10^{-2}$ min^{-1}	0.150	0.178	0.033	0.156
	q_{eq}/mg g^{-1}	7.999	38.38	15.21	21.90
	RSE[a]	1.071	2.581	0.722	0.729
	SSR[b]	17.22	99.94	7.811	7.968
Pseudo-second-order	$k_2/10^{-3}$ g mg^{-1} min^{-1}	0.025	0.009	0.003	0.014
	q_{eq}/mg g^{-1}	8.478	39.73	16.41	22.65
	RSE	0.781	1.294	0.550	0.292
	SSR	9.151	25.10	4.539	1.280
Intraparticle diffusion	k_{id}/mg g^{-1} $min^{-0.5}$	0.401	1.830	0.677	1.032
	l/mg g^{-1}	5.603	26.63	1.470	11.30
	RSE	3.878	21.48	5.949	12.23
	SSR	240.6	7,382	566.3	2,394
Elovich	α/mg g^{-1} min^{-1}	4.169	27.460	4.599	4.534
	β/g mg^{-1}	0.756	2.074	0.434	8.343
	RSE	0.190	2.036	1.608	1.514
	SSR	0.541	62.20	38.80	34.38

[a]Residual squared errors.
[b]Sum of squared residuals.

3.2.3. Effect of adsorbent dose

The influence of increasing adsorbent dose for the adsorption of Cd^{2+} and Hg^{2+} onto MWCNT-COOH and MWCNT-ttpy from aqueous solutions was investigated over a dosage range of 30–400 mg. Fig. 4 shows an increase in the removal efficiency of Cd^{2+} and Hg^{2+} onto MWCNT-COOH and MWCNT-ttpy as the adsorbent mass is increased. An increase in the removal of adsorbates can be attributed to the increase in the surface area and the number of active sites on the adsorbent, as a result of increasing the adsorbent dose [62]. The improved efficiency of MWCNT-ttpy over MWCNT-COOH is seen in Fig. 4, where sorption was greatly enhanced for Cd^{2+} and Hg^{2+} removal. As before, in the case of Cd^{2+}, MWCNT-ttpy exhibits a large improvement over MWCNT-COOH. This can be attributed to the fact that both metal ions are soft acids and are expected to form strong covalent bonds with borderline bases such as nitrogen.

3.2.4. Effect of initial metal ion concentration

The influence of the initial metal ion concentration on the adsorption of Cd^{2+} and Hg^{2+} onto MWCNT-COOH and MWCNT-ttpy was examined over a concentration range of 10–100 mg dm^{-3}. As observed in both cases, an increase in the metal ion concentration, resulted in a decrease in the percentage removal from 38.2% to 16.8% and 97.7% to 88.0% for Cd^{2+}, and 90.0% to 62.9% and 98.8% to 81.9% for Hg^{2+}, onto MWCNT-COOH and MWCNT-ttpy, respectively. The observed decrease is due to the presence of more metal ions in solution, which limits the number of available adsorption sites [15]. This trend, however, yielded an increase in metal ion uptake per unit mass of adsorbent (q_e) with increase in concentration as shown in Figs. 5 and 6. This can be attributed to an increasing number of collisions between the metal ions and active sorbent sites, resulting in higher occupation of the sites at high initial concentrations, and thus high adsorption capacities [15]. As the initial metal ion concentration is increased, the uptake of adsorbates is noticed to reach a plateau where no further increase takes place. This plateau is as a result of the complete occupation of the active sites at a particular concentration, and little or no further increase can occur.

Fig. 5(a) shows that the sorption of Cd^{2+} onto MWCNT-COOH was low compared with MWCNT-ttpy (Fig. 5(b)). This could be as a result of the low affinity of hard oxygen-donor atoms towards soft metals such as cadmium. The enhanced uptake of Cd^{2+} by MWCNT-ttpy could be as a result of the presence of nitrogen-donor atoms on the adsorbent, which act as chelating sites for the adsorbate. Fig. 6 demonstrates that both adsorbents had good efficiency towards the removal of Hg^{2+} over the concentration range studied. Hence, the sorption of Hg^{2+} could be said to be effective by using either oxygen- or nitrogen-containing MWCNTs.

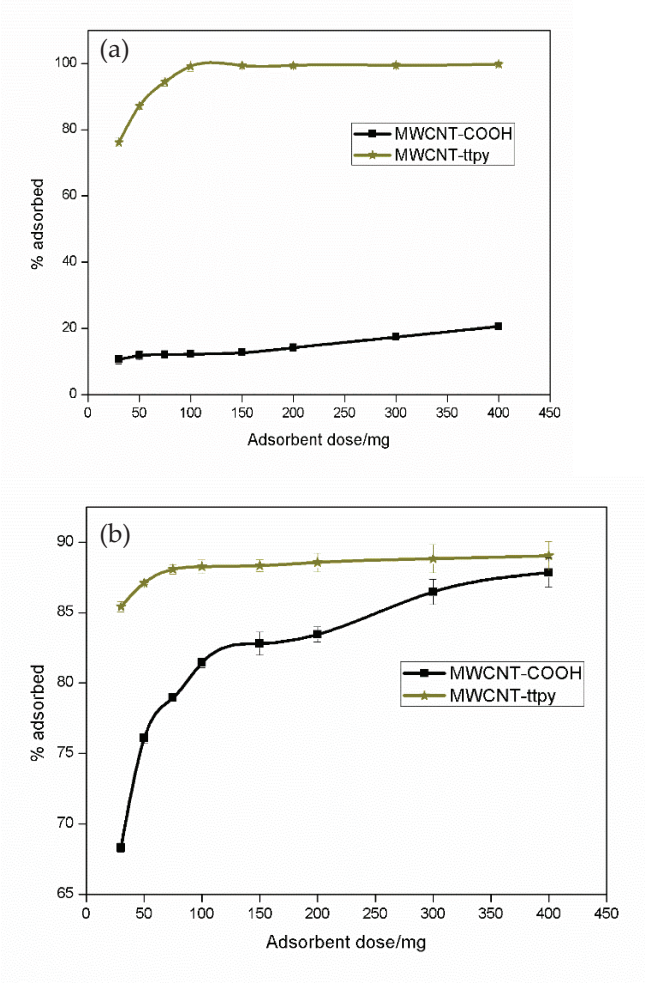

Fig. 4. Effect of adsorbent dose on the adsorption of (a) Cd^{2+} and (b) Hg^{2+} by using MWCNT-COOH and MWCNT-ttpy (conditions: 25 cm^3 of 100 or 50 mg dm^{-3} of Cd^{2+}/Hg^{2+} solution, 24 h equilibration time, pH = 5.5 (Cd^{2+}) and pH = 6.0 (Hg^{2+}), agitation speed 150 rpm and temperature 20°C).

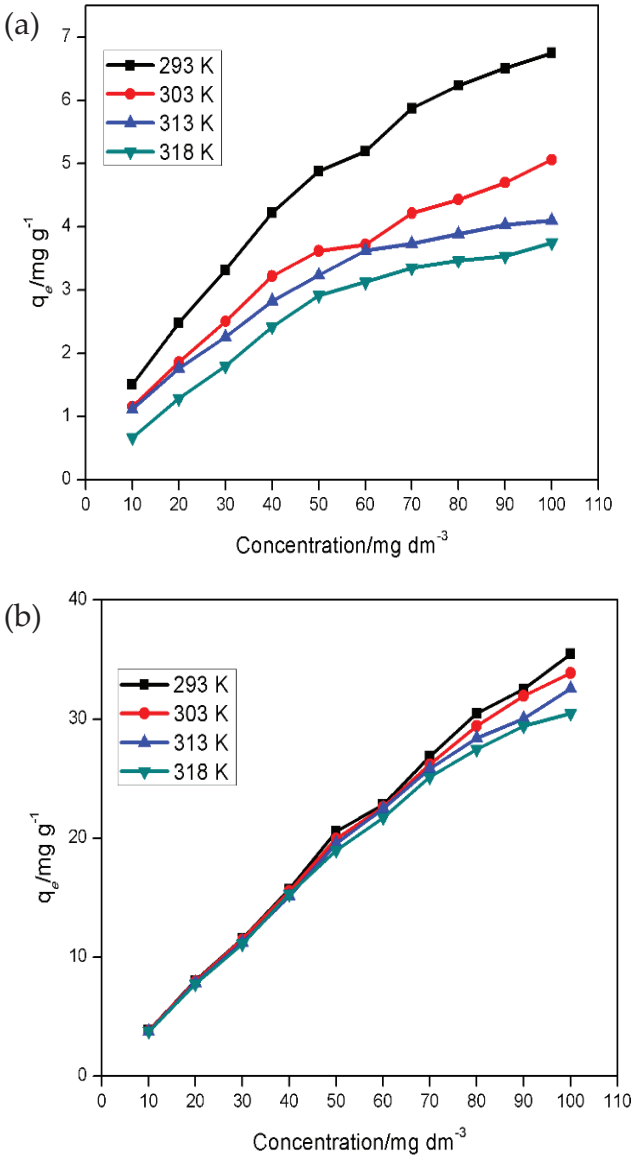

Fig. 5. Effect of temperature on the adsorption of Cd^{2+} onto (a) MWCNT-COOH and (b) MWCNT-ttpy (conditions: 25 cm^3 of Cd^{2+} solution, 24 h equilibration time, 50 mg adsorbent dose, pH = 5.5 and agitation speed 150 rpm).

3.2.5. Effect of temperature

The influence of temperature on the adsorption of Cd^{2+} was studied over a temperature range of 20°C–45°C. However, due to volatility losses which could result in environmental hazards associated with Hg^{2+} at increased temperatures, its temperature effects were examined only at 20°C and 30°C. The sorption of Cd^{2+} onto both adsorbents was noticed to decrease with an increase in temperature (Fig. 5). This is attributed to a decrease in the physical adsorptive forces (van der Waals) and the release of heat between the metal ion and active sites on the adsorbent [15], hence, resulting in a sorption decrease as temperature is increased. The adsorption of Cd^{2+} onto the adsorbents was therefore exothermic in nature. In contrast, Fig. 6 shows an increase in the removal of Hg^{2+} as the adsorbate temperature is increased from 20°C to 30°C. This could be due to volatility losses of Hg^{2+} at increased temperatures, or an increase in the mobility of Hg^{2+} towards the adsorbent sites and an increase in the size of the adsorbent pores [15]. These results are in agreement with inferences drawn by Hadi et al. [15], demonstrating the endothermic nature of adsorption for the removal of Hg^{2+} from aqueous solutions. Similarly, previous studies by Hamza [32], Al Othman et al. [29] and Kumar et al. [33] demonstrated that Cd^{2+} sorption was more favourable at low adsorbate temperature. The thermodynamic parameters, such as enthalpy change, entropy change and change in Gibbs energy for the adsorption of Cd^{2+} were calculated and are discussed in section 3.2.7. However, thermodynamic parameters for Hg^{2+} sorption could not be calculated due to environmental exposure, which could be associated with increased adsorbate temperature, and hence, experiments were performed at only two temperatures from which inferences cannot be drawn.

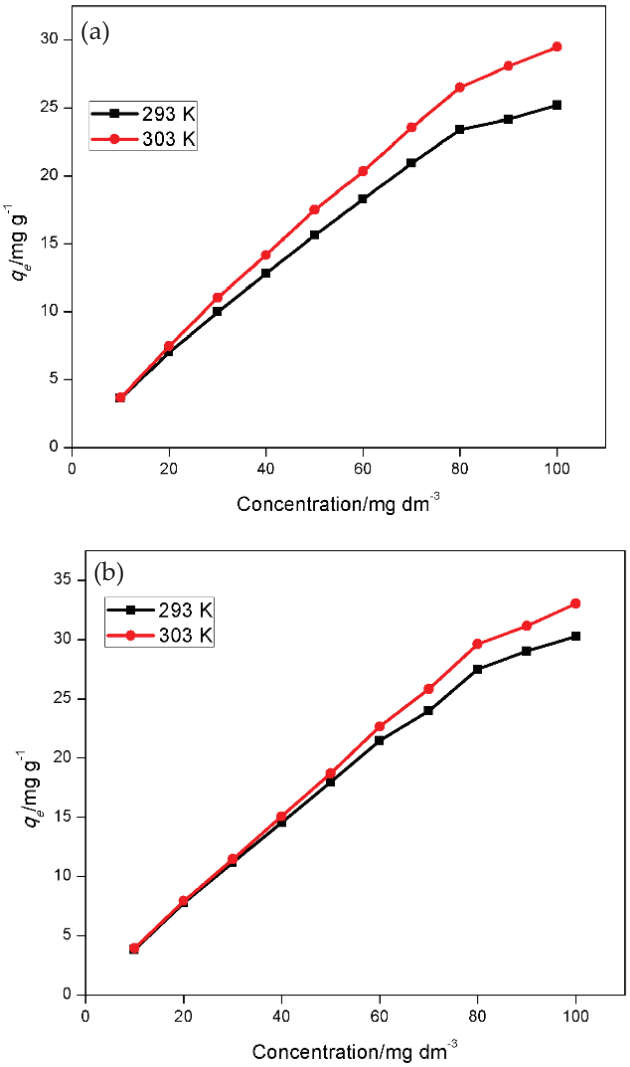

Fig. 6. Effect of temperature on the adsorption of Hg^{2+} onto (a) MWCNT-COOH and (b) MWCNT-ttpy (conditions: 25 cm^3 of Hg^{2+} solution, 24 h equilibration time, 50 mg adsorbent dose, pH = 6.0 and agitation speed 150 rpm).

3.2.6. Isotherm studies

Equilibrium adsorption isotherms are mathematical expressions used to estimate the capacity of an adsorbent for the removal of a targeted pollutant and describe the distribution of species in the solid–liquid phases [8]. Adsorption experiments were performed by adding specific amounts of the adsorbents into aliquots of Cd^{2+}/Hg^{2+} solutions of varying metal ion concentrations ranging from 10 to 100 mg dm^{-3} over a temperature range of 293–318 K for Cd^{2+} and 293–303 K for Hg^{2+}. The equilibrium data obtained were fitted into various two- and three-parameter isotherm models listed in Table 2 and the fit of the models to the experimental data were compared to obtain the isotherms that best describe the adsorption process. The adequacy of a model was decided based on the lowest values for the SSR and the RSE obtained.

Tables 6 and 7 give the isotherm parameters for models which fit the equilibrium data most appropriately for the adsorption of Cd^{2+} and Hg^{2+}, respectively. The Langmuir isotherm was the best two-parameter model that could describe the adsorption of Cd^{2+} onto both sorbents (Table 6). The equilibrium data obtained for MWCNT-COOH could not be described by any of the three-parameter isotherm models, however, data obtained for MWCNT-ttpy were best described by the Redlich–Peterson (R-P) and Sips models.

The data obtained for the sorption of Hg^{2+} onto both adsorbents over a temperature range of 293–303 K were best described by the Langmuir model for the two-parameter isotherms, and the Sips model for the three-parameter isotherms (Table 7).

The Langmuir model is used to describe systems with homogeneous adsorbent surfaces where it is assumed that the adsorbent surfaces contain a finite number of identical sites with uniform energies of adsorption, and hence no interactions exist between adjacent adsorbed species [8,70]. The Freundlich isotherm, however, describes a system where adsorption occurs on multilayer surfaces, containing heterogeneous adsorbent sites. Hence, since the sorption of Cd^{2+} and Hg^{2+} onto MWCNT-COOH and MWCNT-ttpy fit better to the Langmuir model than the Freundlich model, it could be assumed that all sites were equivalent, holding one adsorbate molecule without interactions with adjacent sites [70]. This model has been chosen as an isotherm of choice by other authors such as Wu et al. [8], Perez-Aguilar et al. [2], Kabbashi et al. [17] and Chen et al. [65] for the sorption of Cd^{2+} and Hg^{2+} from aqueous solutions. Of the three-parameter isotherms, the Sips model, which is a combination of the Langmuir and Freundlich models, was chosen to best describe both systems.

A comparison of the maximum Langmuir adsorption capacity (q_m) for MWCNT-COOH and MWCNT-ttpy demonstrates that both sorbents compare favourably with other adsorbents from previous studies (Table 8). The capacity of MWCNT-ttpy was far greater than all other sorbents compared for the removal of Cd^{2+}, while the sorbent also shows a favourable uptake of Hg^{2+} when compared with other related sorbents (Table 8). This therefore shows that the application of MWCNT-ttpy is suitable, obtaining excellent uptakes of Cd^{2+} and Hg^{2+} from aqueous solutions. It is also interesting to note that a better adsorption ability for Cd^{2+} was obtained in this study for MWCNTs functionalized with a N-donor ligand (HO-Phttpy) than when nitrogen was doped into MWCNTs [2]. However, only slight improvement was noticed when MWCNT-ttpy was applied for Hg^{2+} removal compared with MWCNT-COOH.

Additionally, the parameters obtained from the Langmuir model can be used to estimate the favourability of the adsorption process. The constant, separation factor (R_L), can be calculated as given in Eq. (4) [77,78]:

$$R_L = \frac{1}{1 + bC_i} \tag{4}$$

where C_i is the initial Cd^{2+}/Hg^{2+} concentration (mg dm^{-3}) and b is the Langmuir constant obtained from Tables 6 and 7 (dm^3 mg^{-1}). The favourability of the adsorption process can

Table 6
Isotherm parameters for the adsorption of Cd^{2+} onto MWCNT-COOH and MWCNT-ttpy

Isotherms	Parameter	MWCNT-COOH				MWCNT-ttpy			
		293 K	303 K	313 K	318 K	293 K	303 K	313 K	318 K
Langmuir	q_m	10.41	7.503	5.804	6.3026	41.51	39.71	38.89	36.94
	b	0.022	0.022	0.029	0.017	0.558	0.426	0.288	0.250
	RSE[a]	0.121	0.120	0.102	0.138	1.110	0.452	1.080	0.618
	SSR[b]	0.117	0.114	0.084	0.151	9.864	1.631	9.331	3.052
Freundlich	K_F	0.631	0.451	0.507	0.280	–	–	–	–
	n	1.833	1.845	2.091	1.697	–	–	–	–
	RSE	0.200	0.137	0.187	0.450	–	–	–	–
	SSR	0.319	0.150	0.279	0.237	–	–	–	–
Sips	q_m	–	–	–	–	37.36	37.97	34.62	34.31
	b	–	–	–	–	0.635	0.439	0.2745	0.242
	n	–	–	–	–	0.781	0.914	0.7739	0.8627
	RSE	–	–	–	–	0.632	0.315	0.700	0.404
	SSR	–	–	–	–	2.792	0.694	3.429	1.140
R-P	K	–	–	–	–	19.01	15.02	8.932	7.671
	α	–	–	–	–	0.316	0.306	0.1292	0.1323
	β	–	–	–	–	1.154	1.0777	1.194	1.144
	RSE	–	–	–	–	0.804	0.224	0.780	0.255
	SSR	–	–	–	–	4.524	0.3503	4.256	0.4549

[a]Residual squared errors.
[b]Sum of squared residuals.

Table 7
Isotherm parameters for the adsorption of Hg^{2+} onto MWCNT-COOH and MWCNT-ttpy

Isotherms	Parameter	MWCNT-COOH		MWCNT-ttpy	
		293 K	303 K	293 K	303 K
Langmuir	q_m	33.89	37.67	36.13	38.86
	b	0.085	0.146	0.217	0.348
	RSE[a]	0.769	0.545	1.234	2.019
	SSR[b]	4.733	2.376	12.18	32.62
Freundlich	K_F	4.965	7.155	9.263	12.82
	n	2.118	2.162	2.524	2.811
	RSE	1.384	1.564	1.598	2.702
	SSR	15.33	19.57	20.44	58.39
Sips	q_m	37.00	40.47	46.04	42.14
	b	0.090	0.147	0.205	0.341
	n	1.106	1.090	1.37	1.16
	RSE	0.785	0.521	0.919	2.106
	SSR	4.312	1.903	5.912	31.05

[a]Residual squared errors.
[b]Sum of squared residuals.

be estimated depending on the values of R_L. Adsorption is assumed to be favourable if $0 < R_L < 1$, unfavourable if $R_L > 1$, irreversible if $R_L = 0$ and linear if $R_L = 1$ [77]. All R_L values obtained in this study were found to fall between $0 < R_L < 1$, hence adsorption of Cd^{2+} and Hg^{2+} onto MWCNT-COOH and MWCNT-ttpy indicated a favourable adsorption. The smaller the R_L values, the more favourable the process is. The calculated values of R_L obtained for Hg^{2+} produced lower values than those obtained for Cd^{2+}, onto both adsorbents. This may be indicative that the sorption of Hg^{2+} was more favourable than Cd^{2+} sorption.

3.2.7. Thermodynamic parameters of adsorption

The thermodynamic parameters of adsorption, such as, the change in entropy ($\Delta S°$), change in enthalpy ($\Delta H°$) and change in Gibbs energy ($\Delta G°$), were calculated for the removal of Cd^{2+} from aqueous solutions. The calculations could not be done for the adsorption of Hg^{2+} from aqueous solutions due to the limitations of performing experiments at only two temperatures, hence, there was insufficient data to draw inferences. Thermodynamic parameters are calculated to understand the feasibility and spontaneity of the adsorption process. The process is feasible and spontaneous when $\Delta G°$ values are negative. A positive $\Delta H°$ value signifies the process is endothermic and the reverse is an exothermic process.

Table 8
Comparison of the adsorption capacity of Cd^{2+} and Hg^{2+} onto MWCNT-COOH and MWCNT-ttpy with that of other sorbents

Adsorbent	Cd^{2+}	Hg^{2+}	References
MWCNT	5.40	–	[71]
MWCNT (H_2SO_4)[a]	8.60	–	[71]
MWCNT (H_2SO_4/$KMnO_4$)	46.3	–	[71]
MWCNT	1.10	–	[9]
MWCNT (H_2O_2)	2.60	–	[9]
MWCNT ($KMnO_4$)	11.0	–	[9]
MWCNT (HNO_3)	5.10	–	[9]
N-doped MWCNT	9.33	–	[2]
MWCNT	5.62	–	[72]
MWCNT (H_2SO_4)	20.2	–	[72]
MWCNT (HNO_3)	10.9	–	[73]
MWCNT-EDA	25.7	–	[67]
MWCNT	–	84.0	[61]
MWCNT-SH	–	16.9	[62]
MWCNT-SiO_2	–	13.3	[74]
MWCNT	–	25.6	[75]
MWCNT(HNO_3)	–	27.3	[76]
MWCNT	–	5.47	[76]
MWCNT	–	0.36	[65]
MWCNT (HNO_3)	–	0.41	[65]
MWCNT (H_2SO_4/$KMnO_4$)	–	0.42	[65]
MWCNT (H_2SO_4/HNO_3)	10.4	33.4	This study
N-functionalized MWCNT	41.5	36.1	This study

[a]Modifying agents in parentheses.

The change in Gibbs energy is calculated from the expression in Eq. (5) [48,79]:

$$\Delta G^\circ = -RT\ln K \quad (5)$$

where ΔG° is the standard Gibbs energy change (J mol^{-1}), R is the universal gas constant (8.314 J K^{-1} mol^{-1}) and T is the absolute temperature in Kelvin. The value of K was obtained from the product of q_m and b obtained from the Langmuir plot (Table 6) [80,81]. The value of K was corrected to be dimensionless by multiplying by 1,000 [82].

In order to obtain ΔH° and ΔS° values, a linear plot of $\ln K$ against $1/T$ by using the Van't Hoff expression given in Eq. (6), were used. Estimated values of ΔH° and ΔS° were calculated from the slope and intercept of the line, respectively.

$$\ln K = -\frac{\Delta H^\circ}{RT} + \frac{\Delta S^\circ}{R} \quad (6)$$

The values obtained, as given in Table 9, demonstrate that the sorption of Cd^{2+} onto MWCNT-COOH and MWCNT-ttpy

Table 9
Thermodynamic parameters for the adsorption of Cd^{2+} onto MWCNT-COOH and MWCNT-ttpy

Adsorbent	T (K)	ΔG° (kJ mol^{-1})	ΔH° (kJ mol^{-1})	ΔS° (J K^{-1} mol^{-1})
MWCNT-COOH	293	–13.28		
	303	–12.82		
	313	–13.32	–19.56	–78.96
	318	–12.39		
MWCNT-ttpy	293	–24.48		
	303	–24.53		
	313	–24.26	–28.74	–71.72
	318	–24.14		

was both feasible and spontaneous, as indicated by the negative ΔG° values. Similarly, negative ΔH° and ΔS° values were obtained for both sorbents (Table 9), indicating that the sorption of Cd^{2+} onto MWCNT-COOH and MWCNT-ttpy is exothermic in nature and enthalpy-driven. The values of ΔH° obtained show that the heat evolved was in the range for a physisorption (2.1–20.9 kJ mol^{-1}) process [35,83]. This indicates that the process for the removal of Cd^{2+} from aqueous solutions by using MWCNT-COOH was primarily physisorption. The sorption of Cd^{2+} onto MWCNT-ttpy can be assumed to be a physicochemical process, since ΔH° values were higher than the predicted values for a physisorption process [35,83]. However, negative ΔS° values were obtained for Cd^{2+} sorption onto MWCNT-COOH and MWCNT-ttpy. This trend demonstrates a decrease in the disorderliness of the system as the temperature is increased; adsorption onto both sorbents was enthalpy-driven. Hence, thermodynamic studies reveal the spontaneity of the adsorption process and the favourability of the process at low temperatures onto MWCNT-COOH. However, it is important to note that the sorption of Cd^{2+} onto MWCNT-ttpy was less affected by temperature (Fig. 5(b)), indicating the proficiency of the material for Cd^{2+} removal regardless of an increase in temperature.

3.3. Desorption studies

To investigate the regeneration of adsorbents for reuse, desorption experiments were performed on Cd^{2+}/Hg^{2+}-loaded sorbents. In this study, 0.1 mol dm^{-3} HCl was used to desorb the metal ions from the adsorbents. Prior to desorption, the concentration of metal ions on the loaded adsorbents was obtained, and subsequently the loaded materials were agitated for 30 min in contact with 25 cm^3 of eluent. The removal of Cd^{2+} from the adsorbents was effective achieving a percentage removal of 74% and 82% from MWCNT-COOH and MWCNT-ttpy, respectively. The removal of Hg^{2+} from sorbents produced a percentage removal of 92% and 81% from MWCNT-COOH and MWCNT-ttpy, respectively. The choice of eluent was based on previous reports by Hamza [32] and Hamza et al. [80], Vukovic et al. [67], Saber-Samandari and Gazi [84], Rahman et al. [1], Perez-Aguilar

et al. [2] and Srivastava [85] justifying the removal of metal ions by using acidic solutions. The removal of Cd^{2+} and Hg^{2+} from MWCNT-COOH and MWCNT-ttpy proved efficient by using HCl, hence, isolation of the adsorbate and reutilization of the sorbents is a viable option. The application of the sorbents for the removal of metal ions in solution should be economical, preventing the discharge of spent-sorbents and thereby avoiding the discharge of secondary pollutants into the environment.

4. Conclusions

In this study, nitrogen-functionalized multiwalled carbon nanotubes (MWCNT-ttpy) were applied for the removal of Cd^{2+} and Hg^{2+} from aqueous solutions. Their efficiency for metal ion removal was compared with that of acid-functionalized multiwalled carbon nanotubes (MWCNT-COOH), in order to determine which of the two sorbents was more effective.

The results obtained showed that MWCNT-ttpy was much more effective towards Cd^{2+} and marginally more effective for Hg^{2+} than MWCNT-COOH. For Cd^{2+}, a fourfold increase in removal (i.e., 10.41 to 41.51 mg g^{-1}) was achieved by MWCNT-ttpy over MWCNT-COOH. Although, the removal efficiencies of both sorbents towards Hg^{2+} removal were similar, an increase in its uptake was obtained for MWCNT-ttpy. This demonstrates the effectiveness of CNTs functionalized with a nitrogen-donor ligand towards the removal of divalent metal ions in solution. The pseudo-second-order model described the kinetics data most appropriately, indicating a bimolecular chemical interaction between metal cations and the active surface of the adsorbents. Hence, the sorption of Cd^{2+} and Hg^{2+} primarily interacted with the active sites on the adsorbents via coordination (dative covalent bonding) interaction.

Of the two-parameter isotherms tested, the Langmuir model best described the sorption of both adsorbates, while the Sips model was the best of the three-parameter isotherms for the sorption of Cd^{2+} by MWCNT-ttpy and for Hg^{2+} with both adsorbents. An increase in temperature resulted in a decrease in the uptake of Cd^{2+}, indicating that adsorption was favourable at low temperatures. However, the sorption of Hg^{2+} showed an increase in removal with an increase in temperature. This is indicative that the sorbents are effective for Hg^{2+} removal at high temperatures, and can be applied to effluents discharged at above ambient temperatures.

Desorption of both adsorbents from the sorbents also produced good efficiencies, indicating that the sorbates and sorbents can be recovered and recycled for reuse. This study therefore demonstrated that MWCNT-ttpy is a good adsorbent for the removal of metal ions from solution and its application in industry should be further explored.

Acknowledgements

The authors wish to thank the University of KwaZulu-Natal, Durban, for research facilities and a postdoctoral fellowship award to OAO, the University of KwaZulu-Natal Nanotechnology Platform and the National Research Foundation (NRF) for provision of research funding.

References

[1] M. Rahman, S. Gul, M. Ajmal, A. Iqbal, A. Achakzai, Removal of cadmium from aqueous solutions using excised leaves of Quetta pine (*Pinus halepensis* Mill.), Bangladesh J. Bot., 42 (2014) 277–281.
[2] N.V. Perez-Aguilar, E. Muñoz-Sandoval, P.E. Diaz-Flores, J.R. Rangel-Mendez, Adsorption of cadmium and lead onto oxidized nitrogen-doped multiwall carbon nanotubes in aqueous solution: equilibrium and kinetics, J. Nanopart. Res., 12 (2010) 467–480.
[3] M. Mohammadi, A. Ghaemi, M. Torab-Mostaedi, M. Asadollahzadeh, A. Hemmati, Adsorption of cadmium(II) and nickel(II) on dolomite powder, Desal. Wat. Treat., 53 (2013) 149–157.
[4] T. Chen, Z. Zhou, R. Han, R. Meng, H. Wang, W. Lu, Adsorption of cadmium by biochar derived from municipal sewage sludge: impact factors and adsorption mechanism, Chemosphere, 134 (2015) 286–293.
[5] T.A. Saleh, M. Tuzen, A. Sarı, Magnetic activated carbon loaded with tungsten oxide nanoparticles for aluminum removal from waters, J. Environ. Chem. Eng., 5 (2017) 2853–2860.
[6] O.A. Oyetade, A.A. Skelton, V.O. Nyamori, S.B. Jonnalagadda, B.S. Martincigh, Experimental and DFT studies on the selective adsorption of Pb^{2+} and Zn^{2+} from aqueous solution by nitrogen-functionalized multiwalled carbon nanotubes, Sep. Purif. Technol., 188 (2017) 174–187.
[7] K. Kadirvelu, M. Kavipriya, C. Karthika, N. Vennilamani, S. Pattabhi, Mercury(II) adsorption by activated carbon made from sago waste, Carbon, 42 (2004) 745–752.
[8] S. Wu, K. Zhang, X. Wang, Y. Jia, B. Sun, T. Luo, F. Meng, Z. Jin, D. Lin, W. Shen, L. Kong, J. Liu, Enhanced adsorption of cadmium ions by 3D sulfonated reduced graphene oxide, Chem. Eng. J., 262 (2015) 1292–1302.
[9] Y.-H. Li, S. Wang, Z. Luan, J. Ding, C. Xu, D. Wu, Adsorption of cadmium(II) from aqueous solution by surface oxidized carbon nanotubes, Carbon, 41 (2003) 1057–1062.
[10] B.B. Johnson, Effect of pH, temperature, and concentration on the adsorption of cadmium on geothite, Environ. Sci. Technol., 24 (1990) 112–118.
[11] J. Liang, J. Liu, X. Yuan, H. Dong, G. Zeng, H. Wu, H. Wang, J. Liu, S. Hua, S. Zhang, Z. Yu, X. He, Y. He, Facile synthesis of alumina-decorated multi-walled carbon nanotubes for simultaneous adsorption of cadmium ion and trichloroethylene, Chem. Eng. J., 273 (2015) 101–110.
[12] World Health Organization, Guidelines for Drinking-Water Quality, WHO, Geneva, 2008.
[13] World Health Organization, Guidelines for Drinking-Water Quality, WHO, Geneva, 2011.
[14] E. Kopysc, K. Pyrzynska, S. Garbos, E. Bulska, Determination of mercury by cold-vapor atomic absorption spectrometry with preconcentration on a gold-trap, Anal. Sci., 16 (2000) 1309–1312.
[15] P. Hadi, M.H. To, C.W. Hui, C.S. Lin, G. McKay, Aqueous mercury adsorption by activated carbons, Water Res., 73 (2015) 37–55.
[16] D. Mohan, V.K. Gupta, S.K. Srivastava, S. Chander, Kinetics of mercury adsorption from wastewater using activated carbon derived from fertilizer waste, Colloids Surf., A, 177 (2009) 169–181.
[17] N.A. Kabbashi, M. Elwathig, A. AbuSam, I.N. Bt Jamil, Kinetic study on Hg(II) removal by CNT, Prog. Nanotechnol. Nanomater., 4 (2015) 1–6.
[18] Y. Zhang, L. Zhao, R. Guo, N. Song, J. Wang, Y. Cao, W. Orndorff, W.-P. Pan, Mercury adsorption characteristics of HBr-modified fly ash in an entrained-flow reactor, J. Environ. Sci., 33 (2015) 156–162.
[19] Q. Zhou, Y. Duan, C. Zhu, J. Zhang, M. She, H. Wei, Y. Hong, Adsorption equilibrium, kinetics and mechanism studies of mercury on coal-fired fly ash, Korean J. Chem. Eng., 32 (2015) 1405–1413.
[20] The European Parliament and the Council of the European Union, Directive 2011/65/EU of the European Parliament and of the Council of 8 June 2011 on the restriction of the use of certain hazardous substances in electrical and electronic equipment, Off. J. Eur. Union, 174 (2011) 88–110.

[21] L.Y. Blue, P. Jana, D.A. Atwood, Aqueous mercury precipitation with the synthetic dithiolate, $BDTH_2$, Fuel, 89 (2010) 1326–1330.
[22] N. Ratner, D. Mandler, Electrochemical detection of low concentrations of mercury in water using gold nanoparticles, Anal. Chem., 87 (2015) 5148–5155.
[23] A. Elsherief, Removal of cadmium from simulated wastewaters by electrodeposition on spiral wound steel electrode, Electrochim. Acta, 48 (2003) 2667–2673.
[24] C.S. Slater, A. Ferrari, P. Wisniewski, Removal of cadmium from metal processing wastewaters by reverse osmosis, J. Environ. Sci. Health, Part A, 22 (1987) 707–728.
[25] Y.K. Henneberry, T.E.C. Kraus, J.A. Fleck, D.P. Krabbenhoft, P.M. Bachand, W.R. Horwath, Removal of inorganic mercury and methylmercury from surface waters following coagulation of dissolved organic matter with metal-based salts, Sci. Total Environ., 409 (2011) 631–637.
[26] T.S. Anirudhan, L. Divya, M. Ramachandran, Mercury(II) removal from aqueous solutions and wastewaters using a novel cation exchanger derived from coconut coir pith and its recovery, J. Hazard. Mater., 157 (2008) 620–627.
[27] T.A. Saleh, A. Sarı, M. Tuzen, Effective adsorption of antimony(III) from aqueous solutions by polyamide-graphene composite as a novel adsorbent, Chem. Eng. J., 307 (2017) 230–238.
[28] E. Altıntıg, H. Altundag, M. Tuzen, A. Sarı, Effective removal of methylene blue from aqueous solutions using magnetic loaded activated carbon as novel adsorbent, Chem. Eng. Res. Des., 122 (2017) 151–163.
[29] Z.A. Al Othman, A. Hashem, M.A. Habila, Kinetic, equilibrium and thermodynamic studies of cadmium(II) adsorption by modified agricultural wastes, Molecules, 16 (2011) 10443–10456.
[30] D. Mohan, K.P. Singh, Single- and multi-component adsorption of cadmium and zinc using activated carbon derived from bagasse—an agricultural waste, Water Res., 36 (2002) 2304–2318.
[31] C. Xiong, C. Yao, Study on the adsorption of cadmium(II) from aqueous solution by D152 resin, J. Hazard. Mater., 166 (2009) 815–820.
[32] I.A.A. Hamza, Preparation and Evaluation of a Sugarcane Bagasse Multi-Walled Carbon Nanotube Composite for the Adsorption of Heavy Metals from Aqueous Solutions, PhD Thesis, University of KwaZulu-Natal, Durban, South Africa, 2013.
[33] P.S. Kumar, K. Ramakrishnan, S.D. Kirupha, S. Sivanesan, Thermodynamic and kinetic studies of cadmium adsorption from aqueous solution onto rice husk, Braz. J. Chem. Eng., 27 (2010) 347–355.
[34] M.E.I. Ahmed, Selective adsorption of cadmium species onto organic clay using experimental and geochemical speciation modeling data, Int. J. Eng. Sci. Technol., 8 (2016) 128–131.
[35] O.A. Oyetade, V.O. Nyamori, B.S. Martincigh, S.B. Jonnalagadda, Effectiveness of carbon nanotube-cobalt ferrite nanocomposites for the adsorption of rhodamine B from aqueous solutions, RSC Adv., 5 (2015) 22724–22739.
[36] A. Dourani, M. Hamadanian, M. Haghgoo, Morphology and electrical properties of multi-walled carbon nanotube/carbon aerogel prepared by using polyacrylonitrile as precursor, RSC Adv., 5 (2015) 49944–49952.
[37] Y. Li, J. Niu, Z. Shen, C. Feng, Size effect of single-walled carbon nanotube on adsorption of perfluorooctanesulfonate, Chemosphere, 91 (2013) 784–790.
[38] Y. Zhou, B. Wen, Z. Pei, G. Chen, J. Lv, J. Fang, X. Shan, S. Zhang, Coadsorption of copper and perfluorooctane sulfonate onto multi-walled carbon nanotubes, Chem. Eng. J., 203 (2012) 148–157.
[39] Z. Wang, J. Zhao, L. Song, H. Mashayekhi, B. Chefetz, B. Xing, Adsorption and desorption of phenanthrene on carbon nanotubes in simulated gastrointestinal fluids, Environ. Sci. Technol., 45 (2011) 6018–6024.
[40] J.-L. Gong, B. Wang, G.-M. Zeng, C.-P. Yang, C.-G. Niu, Q.-Y. Niu, W.-J. Zhoua, Y. Liang, Removal of cationic dyes from aqueous solution using magnetic multi-wall carbon nanotube nanocomposite as adsorbent, J. Hazard. Mater., 164 (2009) 1517–1522.
[41] G.-C. Chen, X.-Q. Shan, Y.-S. Wang, B. Wen, Z.-G. Pei, Y.-N. Xie, T. Liu, J.J. Pignatello, Adsorption of 2,4,6-trichlorophenol by multi-walled carbon nanotubes as affected by Cu(II), Water Res., 43 (2009) 2409–2418.
[42] O.A. Oyetade, V.O. Nyamori, B.S. Martincigh, S.B. Jonnalagadda, Nitrogen-functionalised carbon nanotubes as a novel adsorbent for the removal of Cu(II) from aqueous solution, RSC Adv., 6 (2016) 2731–2745.
[43] S. Santangelo, G. Messina, G. Faggio, S.H. Abdul Rahim, C. Milone, Effect of sulphuric-nitric acid mixture composition on surface chemistry and structural evolution of liquid-phase oxidised carbon nanotubes, J. Raman Spectrosc., 43 (2012) 1432–1442.
[44] J. Shen, W. Huang, L. Wu, Y. Hu, M. Ye, Study on amino-functionalized multiwalled carbon nanotubes, Mater. Sci. Eng., A, 464 (2007) 151–156.
[45] A.I. Vogel, A Textbook of Quantitative Inorganic Analysis Including Elementary Instrumental Analysis, 3rd ed., Longman, London, 1961.
[46] J. Lin, L. Wang, Comparison between linear and non-linear forms of pseudo-first-order and pseudo-second-order adsorption kinetic models for the removal of methylene blue by activated carbon, Front. Environ. Sci. Eng., 3 (2009) 320–324.
[47] Y.S. Ho, Comment on Cadmium removal from aqueous solutions by chitin: kinetic and equilibrium studies, Water Res., 38 (2004) 2962–2964.
[48] Y.-S. Ho, Removal of copper ions from aqueous solution by tree fern, Water Res., 37 (2003) 2323–2330.
[49] Y.S. Ho, G. McKay, Pseudo-second order model for sorption processes, Process Biochem., 34 (1999) 451–465.
[50] S.H. Chien, W.R. Clayton, Application of Elovich equation to the kinetics of phosphate release and sorption in soils, Soil Sci. Soc. Am. J., 44 (1980) 265–268.
[51] E. Demirbas, M. Kobya, E. Senturk, T. Ozkan, Adsorption kinetics for the removal of chromium(VI) from aqueous solutions on the activated carbons prepared from agricultural wastes, Water SA, 30 (2004) 533–539.
[52] I. Langmuir, The adsorption of gases on plane surfaces of glass, mica and platinum, J. Am. Chem. Soc., 40 (1918) 1361–1402.
[53] H. Freundlich, Adsorption in solids, Z. Phys. Chem., 57 (1906) 385–470.
[54] M.I. Temkin, V. Pyzhev, Kinetics of ammonia synthesis on promoted iron catalysts, Acta Phys. Chim., 12 (1940) 327–356.
[55] M.M. Dubinin, L.V. Radushkevich, The equation of the characteristic curve of activated charcoal, Proc. Acad. Sci. USSR, Phys. Chem. Sect., 55 (1947) 327–329.
[56] R. Sips, Combined form of Langmuir and Freundlich equations, J. Chem. Phys., 16 (1948) 490–495.
[57] J. Toth, State equations of the solid-gas interface layers, Acta Chim. Acad. Sci. Hung., 69 (1971) 311–328.
[58] O. Redlich, D.L. Peterson, A useful adsorption isotherm, J. Phys. Chem., 63 (1959) 1024.
[59] A.R. Khan, I.R. Al-Waheab, A. Al-Haddad, A generalized equation for adsorption isotherms for multi-component organic pollutants in dilute aqueous solution, Environ. Technol., 17 (1996) 13–23.
[60] The R Development Core Team, The R Foundation for Statistical Computing, R version 3.0.2, 2013.
[61] M.J. Shadbad, A. Mohebbi, A. Soltani, Mercury(II) removal from aqueous solutions by adsorption on multi-walled carbon nanotubes, Korean J. Chem. Eng., 28 (2011) 1029–1034.
[62] M. Hadavifar, N. Bahramifar, H. Younesi, Q. Li, Adsorption of mercury ions from synthetic and real wastewater aqueous solution by functionalized multi-walled carbon nanotube with both amino and thiolated groups, Chem. Eng. J., 237 (2014) 217–228.
[63] R.M. Smith, A.E. Martell, Critical Stability Constants, Vol. 6, Plenum Press, New York, 1976.
[64] P. Gans, Hyperquad Simulation and Speciation: HySS, version 4.0.31, 2009.
[65] P.A. Chen, C.-F. Hsu, D.-W. Tsai, Y.-M. Lu, W.-J. Huang, Adsorption of mercury from water by modified multiwalled carbon nanotubes: adsorption behaviour and interference resistance by coexisting anions, Environ. Technol., 35 (2014) 1935–1944.

[66] M.A. Tofighy, T. Mohammadi, Adsorption of divalent heavy metal ions from water using carbon nanotube sheets, J. Hazard. Mater., 185 (2011) 140–147.
[67] G.D. Vukovic, A.D. Marinkovic, M. Coli, M.D. Ristic, R. Aleksic, A.A. Peric-Gruji, P.S. Uskokovic, Removal of cadmium from aqueous solutions by oxidized and ethylenediamine-functionalized multi-walled carbon nanotubes, Chem. Eng. J., 157 (2010) 238–248.
[68] S.G. Muntean, M.E. Radulescu-Grad, P. Sfarloaga, Dye adsorbed on copolymer, possible specific sorbent for metal ions removal, RSC Adv., 4 (2014) 27354–27362.
[69] C.H. Wu, Adsorption of reactive dye onto carbon nanotubes: equilibrium, kinetics and thermodynamics, J. Hazard. Mater., 144 (2007) 93–100.
[70] B. Yu, Y. Zhang, A. Shukla, S.S. Shukla, K.L. Dorris, The removal of heavy metal from aqueous solutions by sawdust adsorption – removal of copper, J. Hazard. Mater., 80 (2000) 33–42.
[71] C.-Y. Kuo, H.-Y. Lin, Adsorption of aqueous cadmium (II) onto modified multi-walled carbon nanotubes following microwave/chemical treatment, Desalination, 249 (2009) 792–796.
[72] H.-H. Cho, K. Wepasnick, B.A. Smith, F.K. Bangash, D.H. Fairbrother, W.P. Ball, Sorption of aqueous Zn[II] and Cd[II] by multiwall carbon nanotubes: the relative roles of oxygen-containing functional groups and graphenic carbon, Langmuir, 26 (2009) 967–981.
[73] Y.-H. Li, J. Ding, Z. Luan, Z. Di, Y. Zhu, C. Xu, D. Wu, B. Wei, Competitive adsorption of Pb^{2+}, Cu^{2+} and Cd^{2+} ions from aqueous solutions by multiwalled carbon nanotubes, Carbon, 41 (2003) 2787–2792.
[74] T.A. Saleh, Isotherm, kinetic, and thermodynamic studies on Hg(II) adsorption from aqueous solution by silica-multiwalled carbon nanotubes, Environ. Sci. Pollut. Res., 22 (2015) 1–11.
[75] K. Yaghmaeian, R.K. Mashizi, S. Nasseri, A.H. Mahvi, M. Alimohammadi, S. Nazmara, Removal of inorganic mercury from aquatic environments by multi-walled carbon nanotubes, J. Environ. Health Sci. Eng., 13 (2015) 1–9.
[76] A. Gupta, S. Vidyarthi, N. Sankararamakrishnan, Enhanced sorption of mercury from compact fluorescent bulbs and contaminated water streams using functionalized multiwalled carbon nanotubes, J. Hazard. Mater., 274 (2014) 132–144.
[77] O. Soon-An, S. Chye-Eng, L. Poh-Eng, Kinetics of adsorption of Cu(II) and Cd(II) from aqueous solution on rice husk and modified rice husk, Electron. J. Environ. Agric. Food Chem., 6 (2007) 764–1774.
[78] F. Krika, N. Azzouz, M.C. Ncibi, Adsorptive removal of cadmium from aqueous solution by cork biomass: equilibrium, dynamic and thermodynamic studies, Arab. J. Chem., 9 (2016) S1077–S1083.
[79] S.O. Akpotu, B. Moodley, Synthesis and characterization of citric acid grafted MCM-41 and its adsorption of cationic dyes, J. Environ. Chem. Eng., 4 (2016) 4503–4513.
[80] I.A.A. Hamza, B.S. Martincigh, J.C. Ngila, V.O. Nyamori, Adsorption studies of aqueous Pb(II) onto a sugarcane bagasse/multi-walled carbon nanotube composite, Phys. Chem. Earth, 66 (2013) 157–166.
[81] R. Djeribi, Q. Hamdaoui, Sorption of copper(II) from aqueous solutions by cedar sawdust and crushed brick, Desalination, 225 (2008) 95–112.
[82] S.K. Milonjić, A consideration of the correct calculation of thermodynamic parameters of adsorption, J. Serb. Chem. Soc., 72 (2007) 1363–1367.
[83] Y. Liu, Y.-J. Liu, Biosorption isotherms, kinetics and thermodynamics, Sep. Purif. Technol., 61 (2008) 229–242.
[84] S. Saber-Samandari, M. Gazi, Removal of mercury(II) from aqueous solution using chitosan-graft-polyacrylamide semi-IPN hydrogels, Sep. Sci. Technol., 48 (2013) 1382–1390.
[85] S. Srivastava, Sorption of divalent metal ions from aqueous solution by oxidized carbon nanotubes and nanocages: a review, Adv. Mater. Lett., 4 (2013) 2–8.